PCCP

COMMUNICATION

View Article Online
View Journal | View Issue

Check for updates

Cite this: *Phys. Chem. Chem. Phys.*, 2025, **27**, 4587

Received 2nd January 2025,
Accepted 10th February 2025

DOI: 10.1039/d5cp00020c

rsc.li/pccp

Puppeteering the reactivity of frustrated Lewis pairs toward CO_2 *via* coordination dichotomy in bridging units†

Mohmmad Faizan and Ravinder Pawar *

***o*-Carborane can be regarded as one of the most versatile bridging units for intramolecular frustrated Lewis pairs (IFLPs) due to the coordination dichotomy of the cage. The acidity and basicity of the active centres can be modulated to control the thermodynamic, kinetic, and mechanistic pathways of the reaction with CO_2 simply by positioning the active centres at different coordination sites on the carborane unit.**

Introduction

Since the first successful application of sterically encumbered Lewis acid and base pairs for the activation of H_2 molecules,[1] various Lewis pairs (*i.e.*, frustrated Lewis pairs (FLPs)) have been investigated for the activation of small molecules such as CO_2.[2–21] Along with the development of new FLPs, to control the kinetics and thermodynamics of their reactions, chemists have also tried to modulate the frustration (*i.e.*, reactivity) of the FLPs by functionalizing the acidic and basic centres with electron-withdrawing and donating groups.[22] Trujillo and Fernandez introduced an innovative approach to control frustration of the FLPs by enhancing the acidity and basicity of active centres through aromaticity.[23,24] The implications of the aromatic modulation on the mechanistic aspects have also been extensively studied recently by us.[25,26] Apart from the modifications at the active centres, the reactivity of the FLPs can also be controlled by restraining the acidic and basic sites *via* appropriate bridging units. This may reduce the entropic factors and immobilize the active centres at an appropriate distance in suitable angles necessary for the highest reactivity.[27,28] For bridged FLPs, known as intramolecular frustrated Lewis pairs (IFLPs), an increase in reactivity toward CO_2 has been observed.[27–29] Jiang *et al.* investigated a series of bridged phosphorus/boron (P/B) IFLPs for the conversion of CO_2 into formic acid.[30] They concluded that IFLPs with longer chains and unsaturated bridging units are more efficient, as these features may provide the proper spatial restriction to the active centres crucial for higher turnover frequency, as reported by Das *et al.*[27]

However, the bridging units that enhance electronic effects at the active sites of IFLPs, along with their optimal immobilization, remain underexplored. Such units could advance IFLP development for CO_2 sequestration. In this regard, *o*-carborane can emerge as an intriguing bridging unit due to its coordination-dependent electronic effects (*i.e.*, coordination dichotomy) within the cage structure (see Scheme 1a).[31–33] It has been found that positioning borane at the carbon atoms of the cage significantly increases its acidity,[34] while adding phosphine at the 9th position creates a highly electron-rich phosphinoborane.[35,36] Thus, *o*-carborane may offer rigid support to active centres and modulate IFLP reactivity. In 2019, Welch and coworkers reported the first Lewis acid- and base-functionalized carborane, 1-Bcat-7-PPh_2-*closo*-1,7-$C_2B_{10}H_{10}$ (where Bcat is catecholylboryl),[37] which cannot be considered as an FLP due to the lack of minimum requirement for frustration. Later, the Xie group introduced the first *o*-carborane-based IFLP (*o*-IFLP), 1-PPh_2-2-BPh_2-1,2-$C_2B_{10}H_{10}$, demonstrating its application in tri-insertion and dearomatization of terminal arylalkynes.[38] Based on these developments, Zhu and colleagues theoretically investigated the dinitrogen activation by the *o*-IFLP.[39] Recently, we have also studied the *o*-IFLP for CO_2 activation.[40] However, the effects of coordination dichotomy in carborane cages on IFLP activity remain unexamined. Thus, in this work, leveraging the electronic effects of *o*-carborane (see Scheme 1a),[31–33] we proposed four unique *o*-carborane-bridged P/B IFLPs for CO_2 activation (see Scheme 1b and Section S1 of the ESI†). In BP, where both acidic and basic sites are located on the electron-withdrawing C1 and C2 atoms, the acidity of $-B(CH_3)_2$ is expected to increase, while the basicity of $-P(CH_3)_2$ may decrease. In BP3, with active sites on the electron-donating B9 and B12 atoms, the reverse is anticipated. For BP1, $-P(CH_3)_2$ at the neutral B5 site likely retains its basicity, with $-B(CH_3)_2$ at the

Laboratory of Advanced Computation and Theory for Materials and Chemistry, Department of Chemistry, National Institute of Technology Warangal (NITW), Warangal, Telangana-506004, India. E-mail: ravinder_pawar@nitw.ac.in

† Electronic supplementary information (ESI) available. See DOI: https://doi.org/10.1039/d4cp00020c

Open Access Article. Published on 10 February 2025. Downloaded on 12/14/2025 6:14:35 AM. This article is licensed under a Creative Commons Attribution-NonCommercial 3.0 Unported Licence.

Open Access Article. Published on 10 February 2025. Downloaded on 12/14/2025 6:14:35 AM.
This article is licensed under a Creative Commons Attribution-NonCommercial 3.0 Unported Licence.

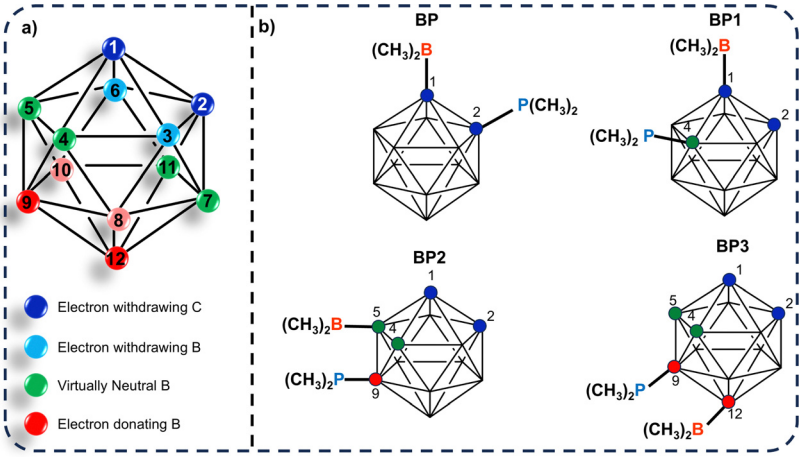

Scheme 1 (a) General structure of *o*-carborane with labels and (b) investigated IFLPs in the present work.

electron-withdrawing C1 site. In BP2, $-B(CH_3)_2$'s acidity should remain unchanged, while the $-P(CH_3)_2$'s basicity may increase as it is positioned on the B9 atom. The expected variations in the acidity and basicity of the active sites can be correlated with the hydride ion affinity (HIA) and proton affinity (PA) of $-B(CH_3)_2$ and $-P(CH_3)_2$, respectively, at various coordination sites given in Table S4 of the ESI.†

The proposed IFLPs were fully optimized at the M062X/Def2TZVP level of theory.[41,42] To validate the anticipated electronic effects on the IFLPs at different coordination sites of the cage, their electronic structures were compared with unsubstituted *o*-carborane using natural bonding orbitals (NBOs) and electron occupancies. The molecular electrostatic potential surface (MESP) of the *o*-carborane, shown in Fig. S1b of the ESI,† reveals the anisotropy of electron density, hence, the coordination dichotomy in terms of maxima (V_{max} = 39.6 kcal mol^{-1}) and minima (V_{min} = −14.48 kcal mol^{-1}) at the cage. NBO analysis shows that an electron withdrawing effect at C atoms results from electron deficit due to the hyper coordinated state of C atoms *via* orbital charge transfer to the bridging B (*i.e.*, B3 and B6) atoms of the cage (see Section S2 of the ESI†). The electron donating ability of the B atoms of the cage arises from the electron excess *via* three centre two electron bonding. The bonding behaviour of the IFLP carborane cage is consistent with that of *o*-carborane (see Section S1 and Tables S1, S2, ESI†), confirming the expected electronic effects at specific sites. Furthermore, quantum theory of atoms in molecules (QTAIM) was employed to analyse electron density around $-P(CH_3)_2$ and $-B(CH_3)_2$ in the IFLPs to assess the impact of coordinating sites on their basicity and acidity.

Electron density plots (Fig. 1) reveal a significant increase in electron density (ρ) at the bond critical point (BCP) X between P and B atoms as the positions of $-B(CH_3)_2$ and $-P(CH_3)_2$ shift from C1 and C2 to B5, B9, and B12 in the IFLPs. In BP ρ at X was 0.0726 which is the lowest among those of all the IFLPs, while in BP3 ρ was found to be the highest. For BP1 and BP2, ρ was 0.0950 and 0.0890, respectively. This indicates that the basicity of $-P(CH_3)_2$ increases due to the electron donating effect of boron atoms of the cage. Furthermore, the fractional percentage changes in BX and PX distances relative to the BP distance in IFLPs indicate the degree of electron density polarization between B and P. In BP, the BX fraction was 34.4% which decreases to 32.6% in BP1 signifying increased electron density transfer from P to B in BP1. Thus, positioning $-P(CH_3)_2$ at the B5 position enhances basicity while maintaining electron deficiency of $-B(CH_3)_2$ at the C1 position. In BP2 and BP3, the BX fraction was found to be ∼33.2%, which was slightly higher than that in BP1. This increase is due to the reduced electron deficiency of $-B(CH_3)_2$, resulting from coordination with the electron-donating B5 or B9 atoms of the cage. Electron density analysis confirms the influence of coordinating sites on the IFLPs' active centres. Although these variations may appear minor, they significantly impact the reaction energetics. Initially the CO_2 molecule interacts with the IFLPs to form reactant complexes (RCs) *via* an interaction between the lone pair orbital of P (lp(P)) and π*(C═O) of CO_2, and the lone pair orbital of O (lp(O)) and empty p_z(B). The orbital charge transfer (OCT) from the lone pair orbital of P (*i.e.*, lp(P)) in the IFLPs and the O atom of CO_2 (*i.e.*, lp(O)) to the π* (C═O) orbital of CO_2 and empty p_z of the B atom of the IFLPs, respectively, is given in Table S3 (ESI†). The lp(P) → π*(C═O) and lp(O) → p_z(B) OCTs range from ∼3 to ∼7 kcal mol^{-1}. Furthermore, the interaction of CO_2 with IFLPs releases the strain imposed by the B–P interaction on the catalysts. The energy released due to this strain removal is also tabulated in Table S3 (ESI†). In BP3 an energy of 4.8 kcal mol^{-1} is released on interaction with CO_2 which is the highest amongst all RCs. The trend in strain release dictates the trend of ΔE in the RCs (see Fig. S3, ESI†) indicating the CO_2 complexation with IFLPs as a strain driven process. Also, due to the complexation, the entropy of the system decreases which leads to the increase in their relative free energy (ΔG) as shown in Fig. S3 (ESI†). The positive (ΔG) signifies that the complexation of CO_2 with IFLPs is an endergonic process which appears in the attainment of the transition state of the reactions. Considering the entropic effects, the energetics of the reactions

 This journal is © the Owner Societies 2025

Open Access Article. Published on 10 February 2025. Downloaded on 12/14/2025 6:14:35 AM.
This article is licensed under a Creative Commons Attribution-NonCommercial 3.0 Unported Licence.

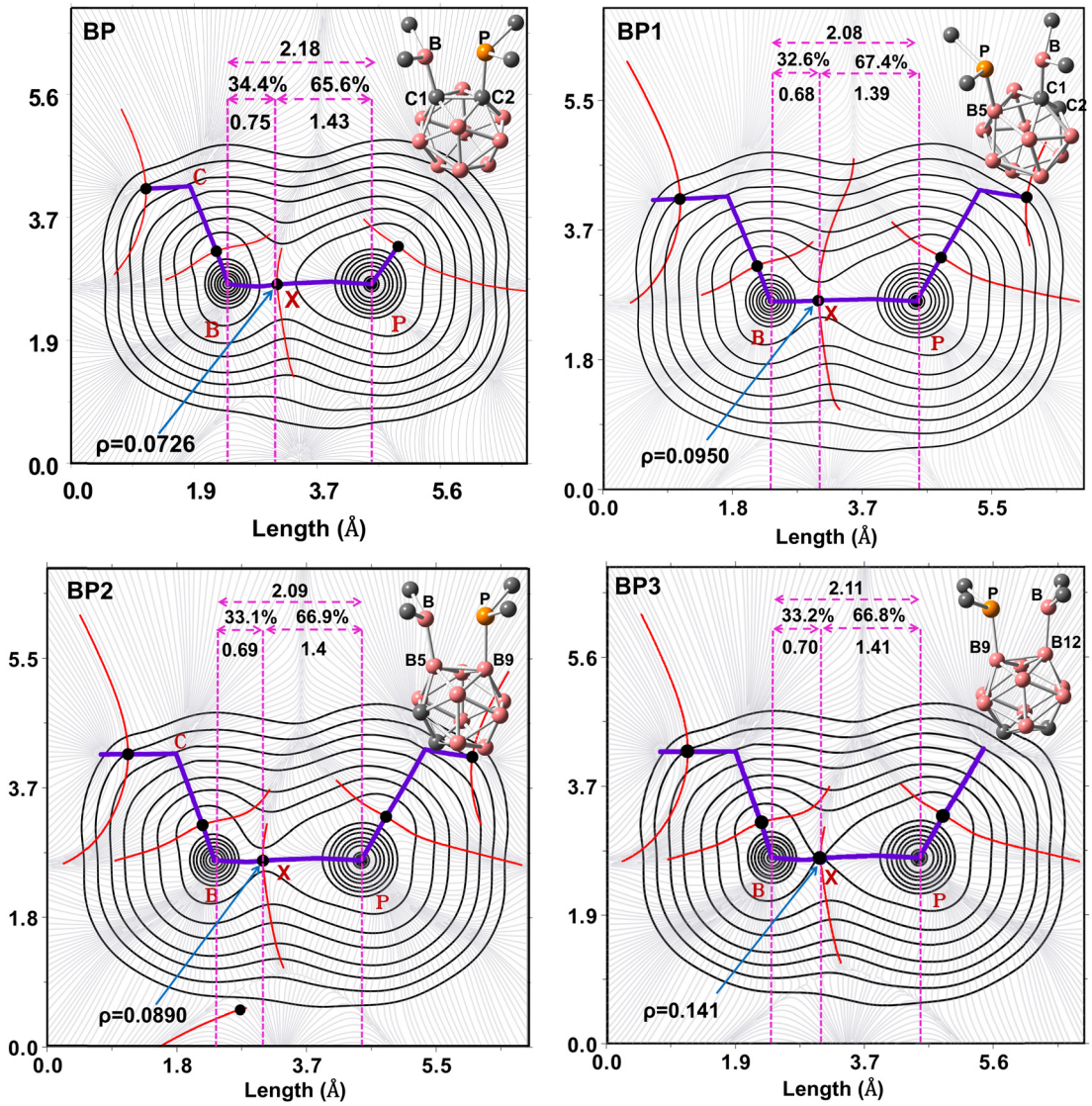

Fig. 1 Electron density plots along with bond critical point (BCP) and inter basin paths between the acidic (B) and basic (P) sites of BP, BP1, BP2 and BP3 along with respective optimized geometries. (The solid circles in black are the BCPs, the red lines are the inter basin paths, purple lines are the paths connecting critical points, X indicates the BCP between B and P, the BP, BX, and XP distances in Å are indicated with magenta arrows with the fractional percentage of distances, and the electron density at X is represented by ρ.)

have been discussed in terms of relative free energies. The relative free energy profile for the reaction of CO_2 with IFLPs is given in Fig. 2 along with labelled optimized structures of the transition states and the formed adducts observed in the reactions.

Fig. 2 illustrates that CO_2 activation in BP requires an activation energy (E_a) of 17.9 kcal mol^{-1}, the highest among those of all the investigated IFLPs. Relocating the $-P(CH_3)_2$ group from the C atom to the B5 position in BP1 reduces the E_a by 6 kcal mol^{-1}. Further repositioning the $-B(CH_3)_2$ and $-P(CH_3)_2$ groups to the B5 and B9 positions, respectively, in BP2 lowers the E_a to 8.7 kcal mol^{-1}. This progressive reduction in E_a with the positional changes of the B and P sites highlights the role of increased basicity in facilitating CO_2 activation. As the basicity of the P site increases upon moving from C to B5 and B9, the interaction between the P atom and the C atom of CO_2 becomes stronger. This is reflected in the enhanced lp(P) $\rightarrow$ π^*(C=O) orbital charge transfer (OCT) values, as shown in Table 1. Conversely, the acidity of the B site decreases, leading to a weaker interaction between the B atom and the O atom of CO_2, evidenced by the reduction in lp(O) $\rightarrow$ p_z(B) OCT from 59.4 kcal mol^{-1} in TSBP to 19.9 kcal mol^{-1} in BP2 (see Table 1). These variations in the electronic interactions are further corroborated by changes in the geometrical parameters of the transition state (TS) structures, providing additional insights into the impact of site-specific modifications on CO_2 activation.

For instance, in TS_{BP} the OCO bond angle was 153.7°, which decreases to 151.7°, 150.3° and 148.3° in TS_{BP1} and TS_{BP2}, respectively, which is accompanied by decreasing PC distances. Also, in TS_{BP} the BO distance was 1.84 Å which subsequently

Open Access Article. Published on 10 February 2025. Downloaded on 12/14/2025 6:14:35 AM.
This article is licensed under a Creative Commons Attribution-NonCommercial 3.0 Unported Licence.

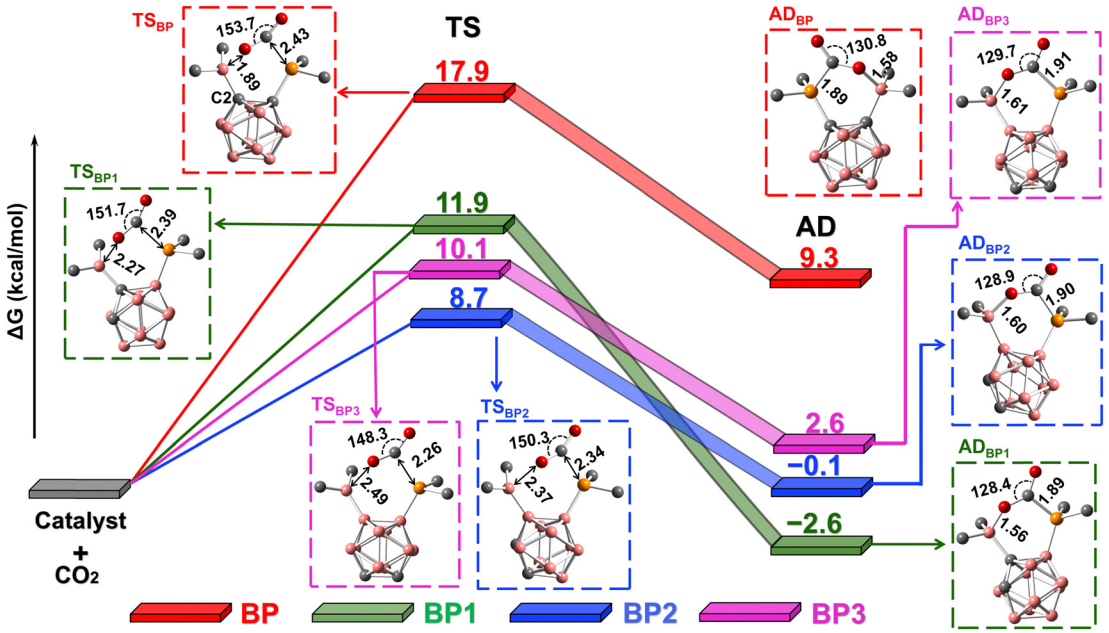

Fig. 2 Relative free energy profile for the reaction of CO_2 with the proposed IFLPs. The optimized geometries of the TSs and ADs obtained in the reactions are given along with appropriate labels and important geometrical parameters (bond distances are in Å and the angles are in degrees, and relative energies are in kcal mol^{-1}).

Table 1 Important orbital charge transfers (OTCs) in the TSs obtained in the reaction of CO_2 with proposed IFLPs (all the values are in kcal mol^{-1})

		lp(P) → π*(C═O)	lp(O) → p_z(B)
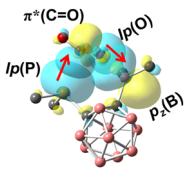	TS_{BP}	124.6	59.4
	TS_{BP1}	163.8	28.9
	TS_{BP2}	195.4	19.9
	TS_{BP3}	257.4	14.7

increased in TS_{BP1}, TS_{BP2} and TS_{BP3}. The increasing BO distances indicate the diminishing B–O interaction in TSs. The changes in P–C and B–O interactions align with the variation in the acidity and basicity of $-B(CH_3)_2$ and $-P(CH_3)_2$ due to the coordination dichotomy of the carborane cage discussed earlier. From these results it can be concluded that the increment in the basicity of the P site on relocation controls the CO_2 activation capacity of the IFLPs where the acidity of the B site is lower. However, when the acidity of the B site is highly enhanced and basicity is significantly reduced (*i.e.*, in BP), the transition state becomes the least stable. Thus, through systematic coordination of active centres on the carborane cage, the reaction kinetics can be effectively controlled. The CO_2 activation energies obtained in all cases are significantly lower than those reported for various bridged IFLPs studied by Jiang and coworkers.[30] In their study, the activation energy for CO_2 ranged from 18 to 36 kcal mol^{-1}, whereas the highest barrier among the IFLPs presented in this work does not exceed 18 kcal mol^{-1}. Additionally, these activation energies are lower than those of aromatically modified P/B IFLPs.[24] Thus, the *o*-carborane bridging unit not only provides effective immobilization of the active site but also introduces significant electronic effects, making it a superior approach for enhancing the reactivity of IFLPs compared to previously investigated methods. Furthermore, as in TSs, the effect of coordinating sites of the carborane can be observed in the relative stabilities of the ADs. In the case of BP1, the acidity of $-B(CH_3)_2$ has been greatly enhanced without any change in the basicity of $-P(CH_3)_2$ giving the most stable adduct AD_{BP1} with a relative energy of −2.6 kcal mol^{-1}. As the acidity decreases, on changing the position of $-B(CH_3)_2$ in BP2 and BP3, the adducts become less stable despite the increment in the basicity of $-P(CH_3)_2$. It is also important to observe that the variation in the stability of the ADs can also be seen from the variation in PC, BO distances and OCO bond angles. Furthermore, in BP where the acidity is significantly increased, the formed adduct (AD_{BP}) was found to be the least stable because of the markedly reduced basicity of $-P(CH_3)_2$. Thus, the stability of the adduct is controlled by the acidity of $-B(CH_3)_2$ with an appropriately basic $-P(CH_3)_2$ group. This indicates that the reaction thermodynamics can also be manipulated by coordinating active centers at different sites of the carborane cage. To better understand the influence of the coordinating sites of the carborane cage on the mechanistic aspects of the IFLPs toward CO_2, the variation of the principal interacting orbital (PIO) based index (PBI)[43,44] along the intrinsic reaction coordinate (IRC) paths was investigated (see Section S1 for details, ESI†).

lp(P)/π*(C═O) and lp(O)/p_z(B) were considered as the 1st and 2nd PIO pairs and the PBI *vs.* IRC plots are divided into different regions based on the inflection in the curves (see Fig. 3). The curve slopes in these regions were analysed to assess the rate of P–C and B–O interactions. It can be observed

 This journal is © the Owner Societies 2025

Open Access Article. Published on 10 February 2025. Downloaded on 12/14/2025 6:14:35 AM.
This article is licensed under a Creative Commons Attribution-NonCommercial 3.0 Unported Licence.

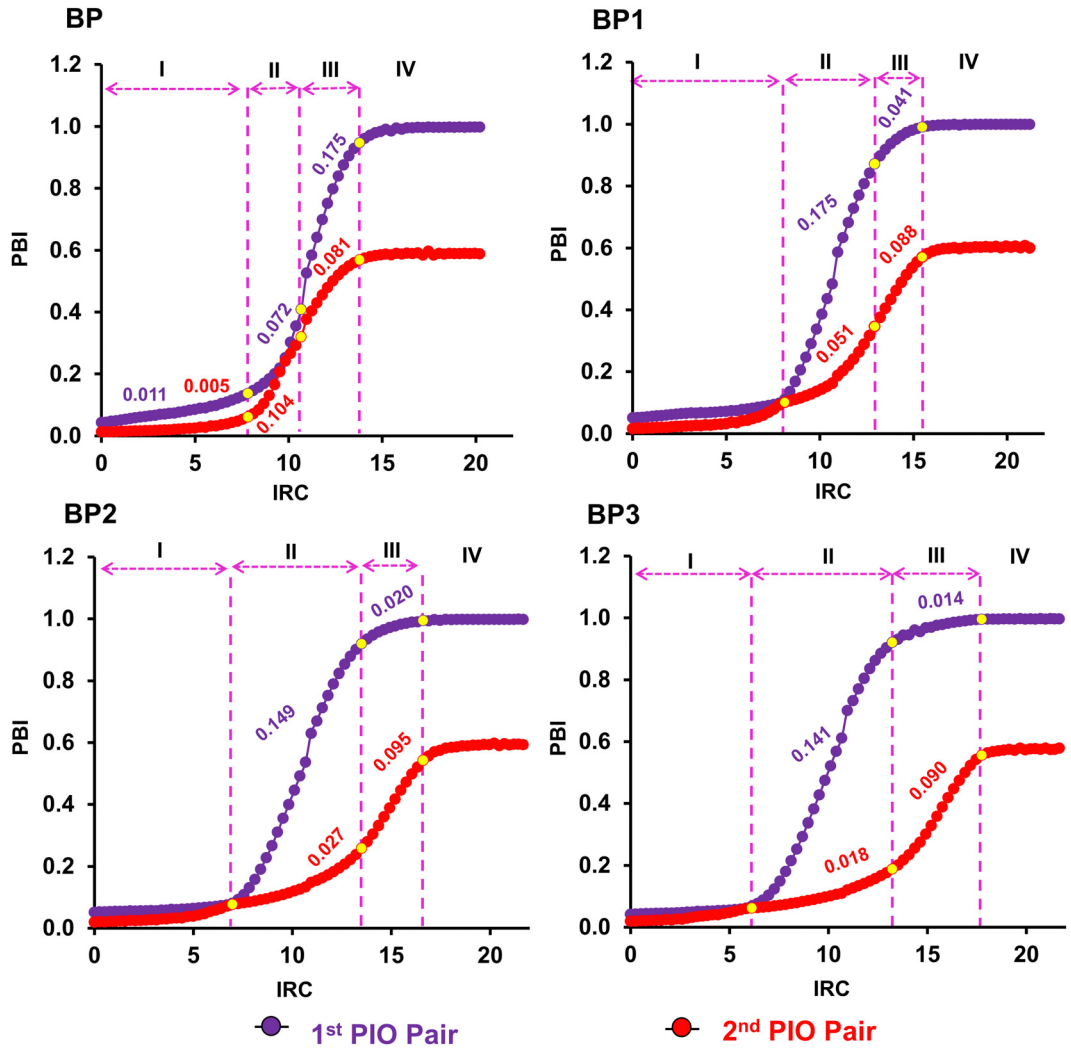

Fig. 3 Variation of the principal interaction orbital (PIO) based index (PBI) along IRC paths for the reaction of CO_2 with the proposed IFLPs (the slopes of the corresponding curves in different regions are given in respective colours; the solid yellow circles represent the point of inflexion in the curves).

from region I of all the IFLPs shown in Fig. 3 that the reaction initiates with P–C interactions, however, as the CO_2 molecule comes into the close vicinity of the reactive site, the reaction mechanism is controlled by the reactivity of the active sites. For instance, in region II of BP the 2nd PIO pair shows a steeper slope than the slope for the 1st PIO pair, while opposite has been observed in the cases of BP1, BP2 and BP3 (see Fig. 3). This suggests that in IFLPs with enhanced basicity, basic sites play a major role in the attainment of the TS. Likewise, in region III of BP the slope of the 2nd PIO pair becomes smaller than the slope of the 1st PIO pair whereas in BP1, BP2 and BP3 the trend is *vice versa*. This shows that in BP the adduct formation is controlled by the basic site while the acidic site controls the adduct formation in other IFLPs. Thus, PIO analysis along the reaction path shows that the reaction mechanism can be controlled by modulating the acidity and basicity through appropriate substitution on the carborane cage which is in accordance with previous understanding of FLPs.[26,45]

In summary, this work introduces *o*-carborane as a novel and versatile bridging unit for IFLPs, enabling control over reaction kinetics and thermodynamics through the coordination dichotomy of the cage structure. DFT calculations show that the acidity and basicity of the active sites can be modulated by adjusting their respective coordination on the carborane cage. IFLPs with an acidic site on the carbon atom of the cage and a basic site on the adjacent B atom form the most stable adduct with moderate activation energy. The use of *o*-carborane as a bridging unit for IFLPs paves the way for the development of a new range of FLPs. We believe that this work will inspire the rational design and development of *o*-carborane-bridged IFLPs for CO_2 sequestration and utilization.

Data availability

All the data supporting the findings of this article are provided in the ESI.†

Open Access Article. Published on 10 February 2025. Downloaded on 12/14/2025 6:14:35 AM. This article is licensed under a Creative Commons Attribution-NonCommercial 3.0 Unported Licence.

Conflicts of interest

There are no conflicts to declare.

Acknowledgements

This work is supported by SERB (EEQ/2023/000424, EEQ/2019/000656 and ECR/2018/002346). With due respect and a sense of obligation we would like to thank NIT Warangal for providing necessary facilities during the research work. One of the authors, M. F., is thankful to the Ministry of Education (MoE), formerly the Ministry of Human Resource Development (MHRD) for providing a Senior Research Fellowship (SRF).

References

1 G. C. Welch, R. R. S. Juan, J. D. Masuda and D. W. Stephan, *Science*, 2006, **314**, 1124–1126.
2 G. Ménard and D. W. Stephan, *J. Am. Chem. Soc.*, 2010, **132**, 1796–1797.
3 F.-G. Fontaine, M.-A. Courtemanche and M.-A. Légaré, *Chem. – Eur. J.*, 2014, **20**, 2990–2996.
4 C. M. Mömming, E. Otten, G. Kehr, R. Fröhlich, S. Grimme, D. W. Stephan and G. Erker, *Angew. Chem., Int. Ed.*, 2009, **48**, 6643–6646.
5 E. Theuergarten, T. Bannenberg, M. D. Walter, D. Holschumacher, M. Freytag, C. G. Daniliuc, P. G. Jones and M. Tamm, *Dalton Trans.*, 2014, **43**, 1651–1662.
6 G. Ménard, T. M. Gilbert, J. A. Hatnean, A. Kraft, I. Krossing and D. W. Stephan, *Organometallics*, 2013, **32**, 4416–4422.
7 A. L. Travis, S. C. Binding, H. Zaher, T. A. Q. Arnold, J.-C. Buffet and D. O'Hare, *Dalton Trans.*, 2013, **42**, 2431–2437.
8 C. Appelt, H. Westenberg, F. Bertini, A. W. Ehlers, J. C. Slootweg, K. Lammertsma and W. Uhl, *Angew. Chem., Int. Ed.*, 2011, **50**, 3925–3928.
9 F. Bertini, V. Lyaskovskyy, B. J. J. Timmer, F. J. J. de Kanter, M. Lutz, A. W. Ehlers, J. C. Slootweg and K. Lammertsma, *J. Am. Chem. Soc.*, 2012, **134**, 201–204.
10 C. Das Neves Gomes, E. Blondiaux, P. Thuéry and T. Cantat, *Chem. – Eur. J.*, 2014, **20**, 7098–7106.
11 B. R. Barnett, C. E. Moore, A. L. Rheingold and J. S. Figueroa, *Chem. Commun.*, 2015, **51**, 541–544.
12 M. Ferrer, I. Alkorta, J. Elguero and J. M. Oliva-Enrich, *J. Phys. Chem. A*, 2021, **125**, 6976–6984.
13 J. J. Chi, T. C. Johnstone, D. Voicu, P. Mehlmann, F. Dielmann, E. Kumacheva and D. W. Stephan, *Chem. Sci.*, 2017, **8**, 3270–3275.
14 S. Maeda and K. Ohno, *Chem. Phys. Lett.*, 2004, **398**, 240–244.
15 Y. Kayaki, M. Yamamoto and T. Ikariya, *Angew. Chem., Int. Ed.*, 2009, **48**, 4194–4197.
16 J. Baltrusaitis, E. V. Patterson and C. Hatch, *J. Phys. Chem. A*, 2012, **116**, 9331–9339.
17 I. Alkorta, C. Trujillo, G. Sánchez-Sanz and J. Elguero, *Inorganics*, 2018, **6**, 110.
18 D. Zhuang, A. M. Rouf, Y. Li, C. Dai and J. Zhu, *Chem. – Asian J.*, 2020, **15**, 266–272.
19 M.-A. Courtemanche, M.-A. Légaré, L. Maron and F.-G. Fontaine, *J. Am. Chem. Soc.*, 2014, **136**, 10708–10717.
20 M. Faizan and R. Pawar, *J. Comput. Chem.*, 2022, **43**, 1474–1483.
21 M. Faizan and R. Pawar, *J. Phys. Chem. A*, 2022, **126**, 8633–8644.
22 R. C. Neu, E. Y. Ouyang, S. J. Geier, X. Zhao, A. Ramos and D. W. Stephan, *Dalton Trans.*, 2010, **39**, 4285.
23 J. J. Cabrera-Trujillo and I. Fernández, *Chem. Commun.*, 2022, **58**, 6801–6804.
24 J. J. Cabrera-Trujillo and I. Fernández, *Chem. Commun.*, 2019, **55**, 675–678.
25 M. Faizan, A. Kumar, M. Raghasudha and R. Pawar, *Phys. Chem. Chem. Phys.*, 2023, **25**, 24809–24818.
26 M. Faizan, M. Chakraborty, D. Bana and R. Pawar, *Phys. Chem. Chem. Phys.*, 2024, **26**, 23609–23622.
27 S. Das, R. C. Turnell-Ritson, P. J. Dyson and C. Corminboeuf, *Angew. Chem., Int. Ed.*, 2022, **61**, e202208987.
28 S. Das, R. Laplaza, J. T. Blaskovits and C. Corminboeuf, *Angew. Chem., Int. Ed.*, 2022, **61**, e202202727.
29 F. Bertini, V. Lyaskovskyy, B. J. J. Timmer, F. J. J. De Kanter, M. Lutz, A. W. Ehlers, J. C. Slootweg and K. Lammertsma, *J. Am. Chem. Soc.*, 2012, **134**, 201–204.
30 B. Jiang, Q. Zhang and L. Dang, *Org. Chem. Front.*, 2018, **5**, 1905–1915.
31 A. M. Spokoyny, C. W. Machan, D. J. Clingerman, M. S. Rosen, M. J. Wiester, R. D. Kennedy, C. L. Stern, A. A. Sarjeant and C. A. Mirkin, *Nat. Chem.*, 2011, **3**, 590–596.
32 V. N. Kalinin and V. A. Ol'shevskaya, *Russ. Chem. Bull.*, 2008, **57**, 815–836.
33 A. Weller, *Nat. Chem.*, 2011, **3**, 577–578.
34 M. O. Akram, C. D. Martin and J. L. Dutton, *Inorg. Chem.*, 2023, **62**, 13495–13504.
35 A. M. Spokoyny, C. D. Lewis, G. Teverovskiy and S. L. Buchwald, *Organometallics*, 2012, **31**, 8478–8481.
36 J. Schulz, R. Clauss, A. Kazimir, S. Holzknecht and E. Hey-Hawkins, *Angew. Chem., Int. Ed.*, 2023, **62**, e202218648.
37 A. Benton, J. D. Watson, S. M. Mansell, G. M. Rosair and A. J. Welch, *J. Organomet. Chem.*, 2020, **907**, 121057.
38 J. Zhang and Z. Xie, *Chem. Sci.*, 2021, **12**, 1745–1749.
39 C. Dai, Y. Huang and J. Zhu, *Organometallics*, 2022, **41**, 1480–1487.
40 M. Faizan, D. Behera, M. Chakraborty and R. Pawar, *ChemPhysChem*, 2024, e202400647.
41 J.-D. Chai and M. Head-Gordon, *Phys. Chem. Chem. Phys.*, 2008, **10**, 6615.
42 S. Grimme, S. Ehrlich and L. Goerigk, *J. Comput. Chem.*, 2011, **32**, 1456–1465.
43 J.-X. Zhang, F. K. Sheong and Z. Lin, *Chem. – Eur. J.*, 2018, **24**, 9639–9650.
44 J. Zhang, F. K. Sheong and Z. Lin, *WIREs Comput. Mol. Sci.*, 2020, **10**, e1469.
45 L. Liu, B. Lukose and B. Ensing, *ACS Catal.*, 2018, **8**, 3376–3381.

 This journal is © the Owner Societies 2025